Inelastic-neutron-scattering study on the acoustical activity of crystals

Shen Zhi-gong and Tao Fang
Institute of Physics, Academia Sinica, P.O. Box 603, Beijing, China

Lin Quan
Chinese Center of Advanced Science and Technology (World Laboratory) P.O. Box 8730, Beijing and Institute of Physics, Academia Sinica, Box 603, Beijing, China

He Chong-fan and Zhou Yi-zhe
Institute of Silicate, Academia Sinica, Shanghai, China
(Received 1 March 1991; revised manuscript received 5 December 1991)

The acoustical-activity effect on dispersion curves has been investigated using inelastic neutron scattering for a series of single crystals. Some interesting phenomena observed in the study of acoustical rotation are summarized. A few empirical formulas are deduced to fit the experimental results. The effects of first-order spatial dispersion on the propagation of sound waves in general directions and a restrictive condition for the gyrotropic effects are demonstrated.

I. INTRODUCTION

Acoustical activity (AA), by analogy with optical activity (OA), is an effect of rotation of the polarization plane of the transverse-acoustic (TA) waves propagating along acoustic axes. It will be observable in those crystal classes possessing axes of threefold or higher symmetry that do not have mirror planes or inversion axes, and results from a decomposition of the linearly polarized modes into right- and left-circularly-polarized (RCP and LCP) modes; the circularly-polarized modes propagate coherently with different velocities and superpose at any point to form a wave linearly polarized at a different angle. The rotated angle of the polarization plane of TA waves in unit propagation distance is called the acoustical rotatory power (ARP).

Early in the 1960's, the concept of AA was introduced into lattice-dynamical theory, and Hooke's law was extended by using a gyrotropic tensor on the assumption that the stress depends not only on the strain, but also on its spatial derivative.[1] Then a phenomenological theory was proposed by Portigal and Burstein (1968, P-B theory) in terms of first-order spatial dispersion and the long-wavelength approximation: A quadratic law of ARP was given, and it was shown that AA could be observed only in eight noncentrosymmetric crystal classes (T, O, C_n, and D_n, $n=3,4,6$). These classes are the same ones that will exhibit OA for light waves propagating along an optic axis.[2] After this, it was theoretically determined that the pure-mode axes having twofold or higher rotational symmetry remain pure when spatial dispersion is present, while the axes that are normal to a mirror plane or a sixfold axis may no longer be pure modes under this condition.[3] This means that AA does not change an acoustic axis into a nonpure mode axis, but would only change it into a nondegenerate one. It was also pointed out that ARP for waves traveling along acoustic axes may undergo a switching of sign, a finite discrete jump in magnitude, or both, when a suitable driving force (electric field or uniaxial stress) is applied.[4] Although many theoretical works followed,[5] real progress had not been made. In 1987, a development was achieved by Li and Chen. They attributed the deviation from the PB theory to the anharmonic interactions using many-body techniques and suggested that AA is closely related to the helix structures of the crystal.[6]

On the experimental side, the nondegeneracy of velocity at a finite wave vector k was found by change in a neutron measurement on the α-SiO_2 crystal (1967).[7] Soon afterwards, its AA at room temperature (RT) was observed directly and investigated by Pine *et al.* with Brillouin-scattering, Raman-scattering, and standard microwave ultrasonic techniques.[8] They obtained the experimental values of the velocity splitting ($\Delta V=V_+-V_-$) and its ARP; they found that ΔV is proportional to the incident frequency ν, that ARP obeys a ν^2 law in the frequency range of 1.05–1.40 GHz, and that the sense of rotation of AA is opposite to that of OA in α-SiO_2. Then, an ultrasonic measurement at 4 K in the range of 8.9–9.17 GHz and a time-of-flight measurement of short pulses of hypersound at RT and 9.425 GHz were accomplished, and similar results were obtained.[9] The degeneracy splitting of TA branches was also found experimentally in single crystals of Te and Se.[10] In 1980, neutron-scattering measurements were used specifically in the study of AA in α-SiO_2 and $NaClO_3$ by Joffrin *et al.*;[11] they demonstrated a q^2 law of frequency splitting ($\Delta\nu=\nu_+-\nu_-$) in a rather wide regime of the reduced wave vector q.

An explanation of why the progress of this subject is slow may be that the direct measurement of AA is more difficult than that of OA. However, AA can be indirectly observed by measuring the splitting in dispersion curves, and so inelastic neutron scattering is found to be useful. Using this method, we have studied the acoustical activity of the single crystals α-SiO_2, $Bi_{12}GeO_{20}$, $Bi_{12}SiO_{20}$, $NaBrO_3$ $NaClO_3$, $NaBr_{0.7}Cl_{0.3}O_3$, Te, TeO_2, $KLiSO_4$, and α-$LiIO_3$.

II. EXPERIMENTAL CONSIDERATIONS AND RESULTS

All measurements were made at RT on a triple-axis spectrometer, which was mostly operated in its constant-momentum-transfer mode and sometimes in the constant-energy mode. The spectrometer was arranged in a W configuration and the $(-\nu,-q)$ combination was generally chosen to achieve a high resolution. A monochromator, either pyrolytic graphite (24′) or hot pressed germanium (27′), and a graphite (30′) analyzer were used to obtain the fixed incident neutron energy at 13.74 or 17.07 meV; for better energy resolution, the monochromator reflection plane was either the (002) plane of graphite or the (111) plane of germanium, while the (004) plane was chosen as the reflecting plane of the analyzer. Ample attention was paid to the spurious peaks and a graphite (36′) filter was often used to eliminate the possible contamination in the incident neutron beams. The horizontal resolution of the Soller collimators between all crystal pairs was 40′. The specimens used in measurements consisted of single crystals oriented usually with the [010] direction perpendicular to the scattering planes.

In addition, it is known that the effect of AA, which is also called circular birefringence, could be massed by a linear birefringence that is associated with crystal defects and misalignment of the wave vector relative to an acoustic axis; that is, two degenerate TA modes split apart linearly as one moves off the acoustic axis. Therefore, great care was given to the perfection of crystals measured and the effect of misalignment in our experiments. The rocking curves and Bragg reflections from different crystallographic planes showed Gaussian peaks and no indication of twinning; for each of two planes of reference, which were chosen to adjust the orientation of crystals measured by using a special goniometer, the relative difference of reflection intensities of the positive face (I_{π}) and the negative face ($I_{-\pi}$) were quite small after repeated adjustments: usually $|(I_{\pi}-I_{-\pi})/I_{\pi}|\sim 1-3\%$. Then, for the same reciprocal-lattice point which was selected as neutron reflection planes, Bragg scans along different directions in reciprocal space were made to determine the position of the $\Gamma(q=0)$ point. The difference of the positions (Δq) observed in these scans is usually less than 0.001. After collecting a set of dispersion data, in order to prove these results, we often chose other reciprocal-lattice points and changed the so-called $(-\nu,-q)$ combination into another combination, say $(+\nu,+q)$ scan, and the geometry of the triple-axis spectrometer from W configuration to another one, as well as the scanning modes from constant-Q scan to constant-E scan, and so on. Finally, we also refixed the crystal measured and readjusted its orientation by using other equivalent or inequivalent planes at which scattering occurred [e.g., substitute the (100) plane or the $(1\bar{1}0)$ plane of cubic crystals for the (010) plane, where its two planes of reference may be changed]. Even the sample was cut in smaller pieces, and neutron data were collected again to prove further their correctness and reliability. All of the results obtained under different conditions above are generally in good agreement with each other.

Our experimental findings may be summarized as follows:

(i) Some neutron groups measured in the [001] and [111] directions are shown in Fig. 1, where lines are hand drawn through the experimental points; TAm ($m=1,2$) and LA denote the transverse- and longitudinal- acoustical phonons, respectively; the peaks below are obtained by the least-squares fitting; the resolution of the spectrometer is illustrated by the full width at half peak. Along these directions only one degenerate TA peak should be detectable in a single scan for normal crystals. However, we obtain simultaneously two individual TA peaks, which are LCP and RCP phonons. They cannot be resolved from each other when the splitting, which increases gradually with q or the average frequency $[\bar{\nu}=(\nu_{+}+\nu_{-})/2]$, is smaller than the resolution of the spectrometer. The data fitted by least squares show that the spectral widths of LCP and RCP phonons are different. Generally, the width of TA1 one is smaller than that of TA2, which is definitely greater than the resolution of the spectrometer within experimental uncertainty. For linearly polarized phonons, the broadening of the energy (or momentum) in neutron peaks indicates that they have a limited lifetime (or propagation length limit). This rule should apply to circularly-polarized phonons, and so a rate of attenuation is found here. It seems that this decay is independent of q and different for different crystals. The order of magnitude of the lifetime was estimated to be $\sim 10^{-11}-10^{-12}$s. It was also shown that the integrated scattering cross section of circularly-polarized phonons obeys the same rule as the linearly-polarized ones (see Ref. 12).

(ii) The dispersion curves of the crystals measured are shown in Fig. 2, where the accuracy of data points is $\sim 4\%$, and smooth lines are hand drawn through these points to show their connectivity. Evidently, the TA branches are no longer degenerate in the regime of $q>0$, and their split shapes are varied. The lower TA branches of most crystals measured (the two TA branches of $NaBrO_3$ as well) are nearly a straight line extending through to the origin within experimental uncertainty; their upper TA branches are gradually bending up when q is small. With further increase of q, they are mostly bending down again; only the upper branches of TeO_2 and the [111] direction of $NaClO_3$ retain the original tendency. On the contrary, the lower TA branches of the [001] direction of $NaClO_3$ and Te are gradually bending down as q goes up to the Brillouin zone boundary, while their upper ones are nearly a straight line, except that the upper branch of Te is gradually bending down when $q>0.1$. Moreover, we find that the magnitude of $\Delta\nu$ and its change with q or $\bar{\nu}$ are very different from each other in the crystals measured, even if they have the same space group (see Table I). The $\Delta\nu$ versus q^2 or $\bar{\nu}^2$ curves are shown in Fig. 3, where all symbols are the experimental points, except the crosses which come from the fitted data. A quadratic law of $\Delta\nu$ ($\Delta\nu=bq^2$ or $b\bar{\nu}^2$) is shown for most crystals measured in different ranges. It holds in the whole Brillouin zone for $NaClO_3$ and TeO_2. For other crystals this law holds only for small q or $\bar{\nu}$ ($q<0.1$ or $\bar{\nu}<0.8$, 0.35, and 0.5 THz, respectively, for α-SiO_2,

$Bi_{12}GeO_{20}$ and Te). With further increase of q or $\bar{\nu}$, their $\Delta\nu$ versus q^2 or $\bar{\nu}^2$ curves will deviate from a straight line (bending downward). Mostly, this deviation leads quickly to a tendency towards "saturation" (i.e., the value of $\Delta\nu$ remains constant for larger q or $\bar{\nu}$). However, it is achieved with the rate which is approximately linear as q goes up to the Brillouin-zone boundary for Te; no saturation occurs. For $NaBrO_3$, saturation is gradually reached after experiencing a linear change of $\Delta\nu$ with q or $\bar{\nu}$, and not even a short section of its $\Delta\nu$ curve conforms to this quadratic law in the range covered by neutron-scattering experiments. A similar AA behavior is exhibited in $NaBr_{0.7}Cl_{0.3}O_3$, whose $\Delta\nu$ curve is slightly lower than that of $NaBrO_3$ and obviously higher than that of $NaClO_3$ in both the [001] and [111] directions, which means that $NaBrO_3$ and $NaClO_3$ with identical chirality have opposite senses in their AA (see Ref. 13). In addition, the magnitudes of $\Delta\nu$ for the 2_1 axes of cubic crystals are always smaller than those for 3_1 or 3_2 axes at the same q. However, the $\Delta\nu$ curves along the threefold screw axes of SiO_2 and Te are situated above that along the fourfold axis of TeO_2 in uniaxial crystals. It is also shown that in $Bi_{12}GeO_{20}$ a small difference is produced by the substitution of Si for Ge, where the atoms lying on special positions on threefold screw axes are Bi and O. However, the replacement of Cl by Br in $NaClO_3$ results in a remarkably different AA behavior, where the helix axes consist of Cl (or Br) and O. So far AA has been observed only along screw axes of the crystals measured (see Table I). The splitting has not been found along the [001]

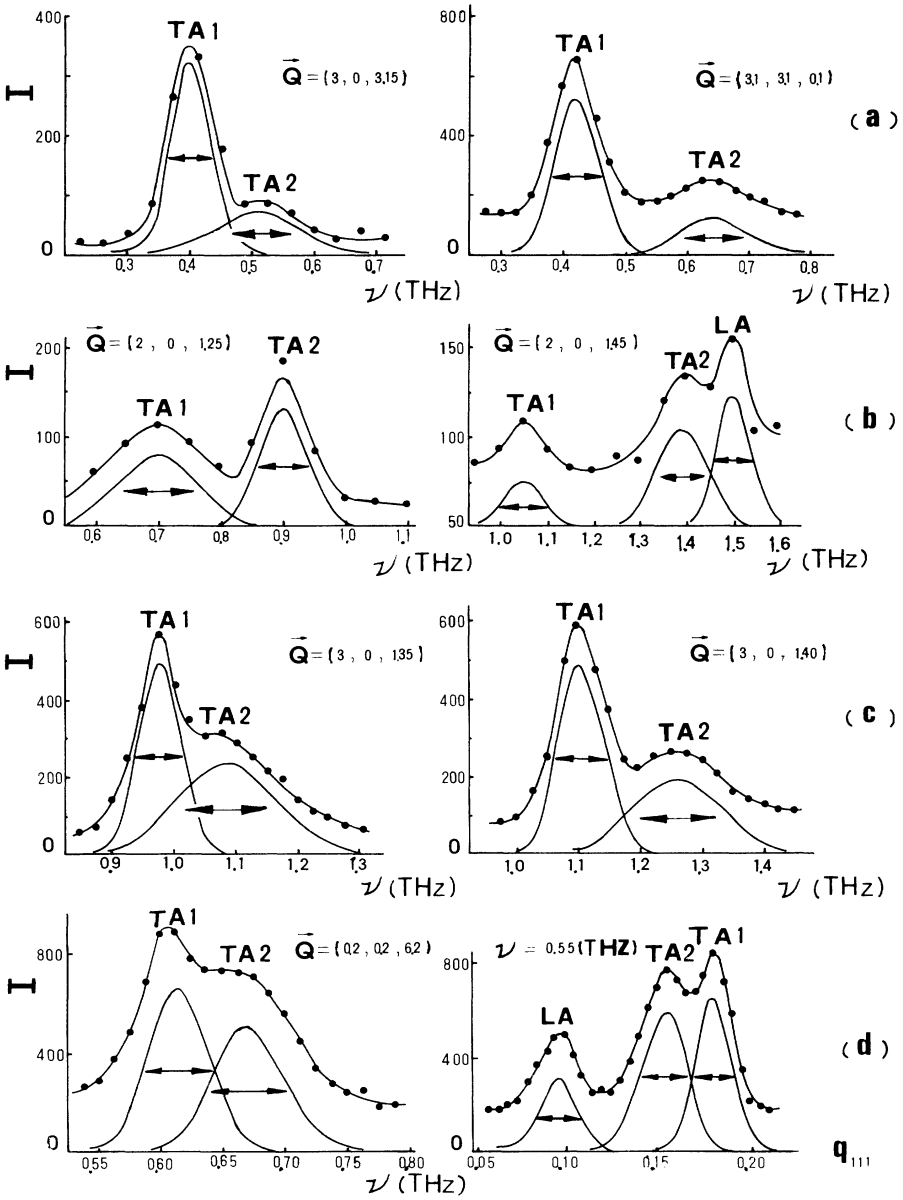

FIG. 1. Some experimental neutron groups from $NaBrO_3$ (a), Te (b), TeO_2 (c), and $Bi_{12}GeO_{20}$ (d), as well as their fitted results.

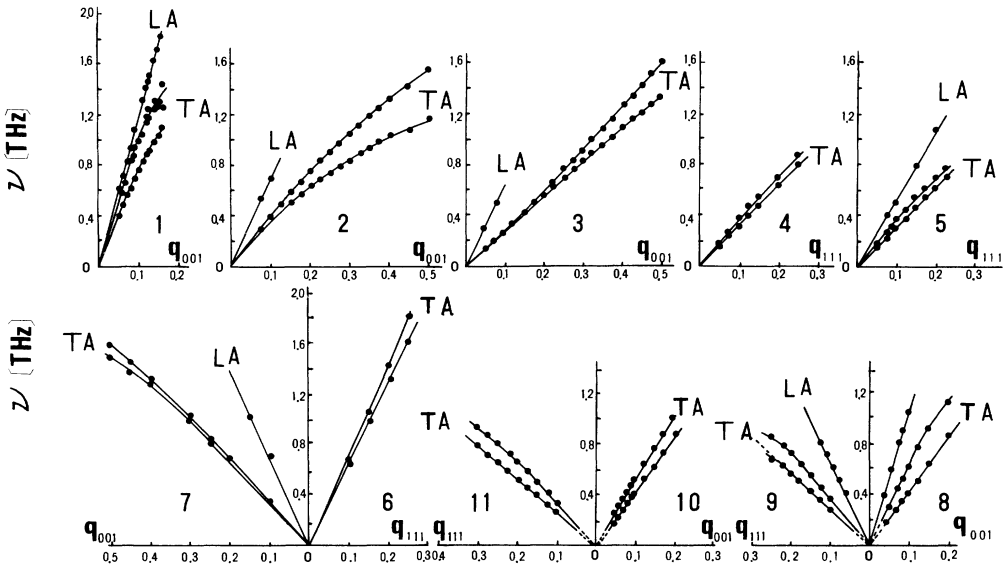

FIG. 2. Experimental dispersion curves in α-SiO_2 (1), Te (2), TeO_2 (3), $Bi_{12}SiO_{20}$ (4), $Bi_{12}GeO_{20}$ (5), $NaClO_3$ (7,6), $NaBrO_3$ (9,8), and $NaBr_{0.7}Cl_{0.3}O_3$ (11,10), where the first curve numbers indicate the [001] direction of the crystals measured and the second ones indicate their [111] directions.

direction of $Bi_{12}GeO_{20}$ up to $q=1.0$, which is a twofold rotation axis without helicity; it is also not found along the 6_3 axes of $KLiSO_4$ and α-$LiIO_3$, which definitely exhibit OA.

(iii) According to the empirical formula deduced in the next section, we have obtained ARP curves of all crystals measured, $R(q^2)$ or $R(\bar{\nu}^2)$, in the range where the quadratic law of $\Delta\nu$ holds. They are shown in Fig. 4. These curves exhibit analogous characters to the $\Delta\nu$ curves; and the larger the $\Delta\nu$, the larger the R is at the same q or $\bar{\nu}$ for different crystals. But the quadratic law of ARP holds approximately only in a much smaller range than the corresponding range of $\Delta\nu$ ($q<0.001$ or $\bar{\nu}<0.01$ THz for SiO_2, Te, and $Bi_{12}GeO_{20}$, $q<0.01$ or $\bar{\nu}<0.1$ THz for $NaClO_3$, and $q<0.2$ or $\bar{\nu}<0.7$ THz for TeO_2); and ARP is not directly proportional to $\Delta\nu$, except that q or $\bar{\nu}$ approaches zero. For $NaBrO_3$ and $NaBr_{0.7}Cl_{0.3}O_3$, in which the quadratic law of $\Delta\nu$ is not found, their ARP as

TABLE I. Experimental values of b and d.

Crystal	α-SiO_2	Te	TeO_2	$NaClO_3$		$Bi_{12}GeO_{20}$
No.	1	2	3	7	6	5
Space group	D_3^4-$P3_121$ D_3^6-$P3_221$		D_4^4-$P4_12_12$ D_4^8-$P4_32_12$	T^4-$P2_13$		T^3-$I23$
Axes	[001]	[001]	[001]	[001]	[111]	[111]
b	28.51	3.85	1.08	0.46	2.52	5.97
b_0 (THz)	10.91	−2.21	0.01	−2.01	2.07	2.08
b_1	8.34	3.99	2.95	3.57	6.53	3.31
b_I	8.67	3.79	2.79	3.30	6.56	3.44
$\bar{b}$ (1/THz)	0.37	0.26	0.12	0.05	0.06	0.52
b/b_1^2	0.38	0.27	0.14	0.04	0.06	0.50
d (10^3 g/s^2)	16.2[a]	3.0	1.3	0.2	0.4	6.1

[a] The values obtained by Brillouin scattering and ultrasonic technique in α-SiO_2 are 14.4 and 13.1 (10^3 g/s^2), respectively.

a function of could be estimated roughly by the linear slopes of their split curves ($V_{\pm}$) in a suitable limit of $\bar{\nu}$. The status of Te is similar for larger ν (see Table II). These results are shown by the dot-dashed lines in Fig. 4(b) in order to make a comparison with the other crystals. In addition, we have also made a few numerical comparisons between the average sound velocity $\bar{V}$ observed by using neutron-scattering technique in a suitable limit of q, in which the slope of split curves may be roughly estimated by that of a straight line ($V_{\pm}$) [i.e., $\bar{V}=(V_+ + V_-)/2$], and the velocity V_T calculated from the relative elastic constants $C_{i,j}$ $(i,j=1,2,4)$ obtained in standard microwave ultrasonic experiments ($V_T^2=C/\rho$), as well as the average velocity splitting $\Delta\bar{V}$ observed in this suitable limit of q [i.e., $\Delta\bar{V}=(V_+ - V_-)/2$] and the velocity splitting (ΔV_P) deduced from the PB theory [i.e., $\Delta V_P = dk/2(\rho C)^{1/2}$, see the discussions below in detail]. These results are shown in Table III. They manifest that the velocity splittings observed in the regime of small q for most crystals measured are in agreement with the PB theory.

(iv) The effect of spatial dispersion on sound velocity has been measured in the [100] direction of TeO_2 and in the [110] direction of $NaClO_3$, $NaBrO_3$, $Bi_{12}GeO_{20}$, and GaAs. Some small changes seem to have been observed in comparison with the values calculated with the absence of spatial dispersion, but they are not definite because this effect in nondegenerate directions is too weak and probably smeared by the experimental uncertainty.

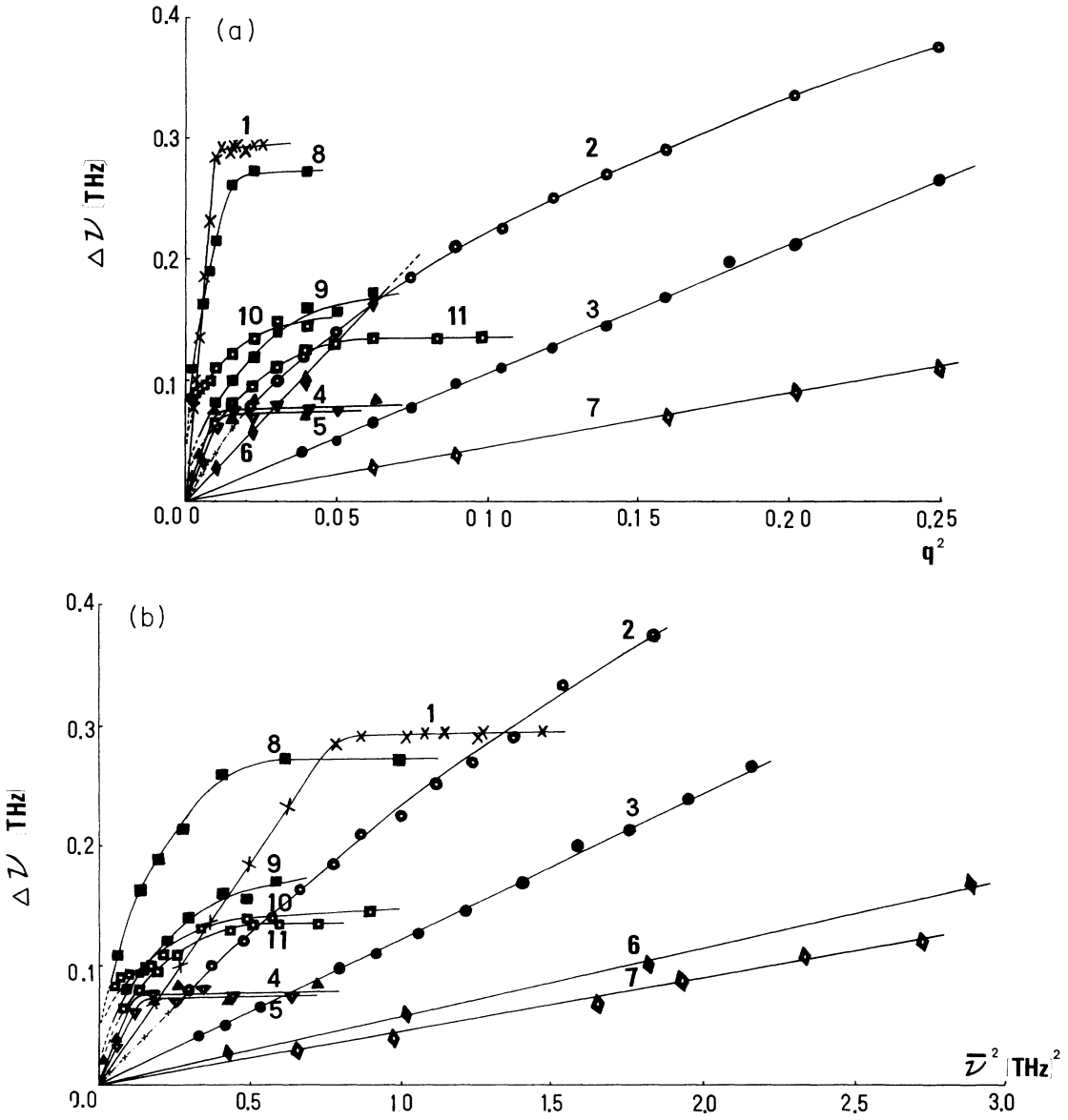

FIG. 3. Experimental frequency-splitting curves as a function of q^2 (a) or $\bar{\nu}^2$ (b), in which the curve numbers stand for the same crystals as those in Fig. 2.

III. DISCUSSION

(a) The macroscopic response of a crystal to an acoustic wave is determined by its elastic constants, which exhibit a dependence on both the temporal and spatial dispersions if the interaction between stress and strain is nonlocal. When the magnitude of the nonlocal part of elastic constants is small, it can be written in a contracted notation as

$$C_{ij}(\omega,\mathbf{k})=C_{ij}(\omega)+id_{ij,l}(\omega)k_l + e_{ij,lm}(\omega)k_lk_m+\cdots , \quad (1)$$

where Voigt's notation of indices $i,j,=1,2,\ldots,6$ is used;

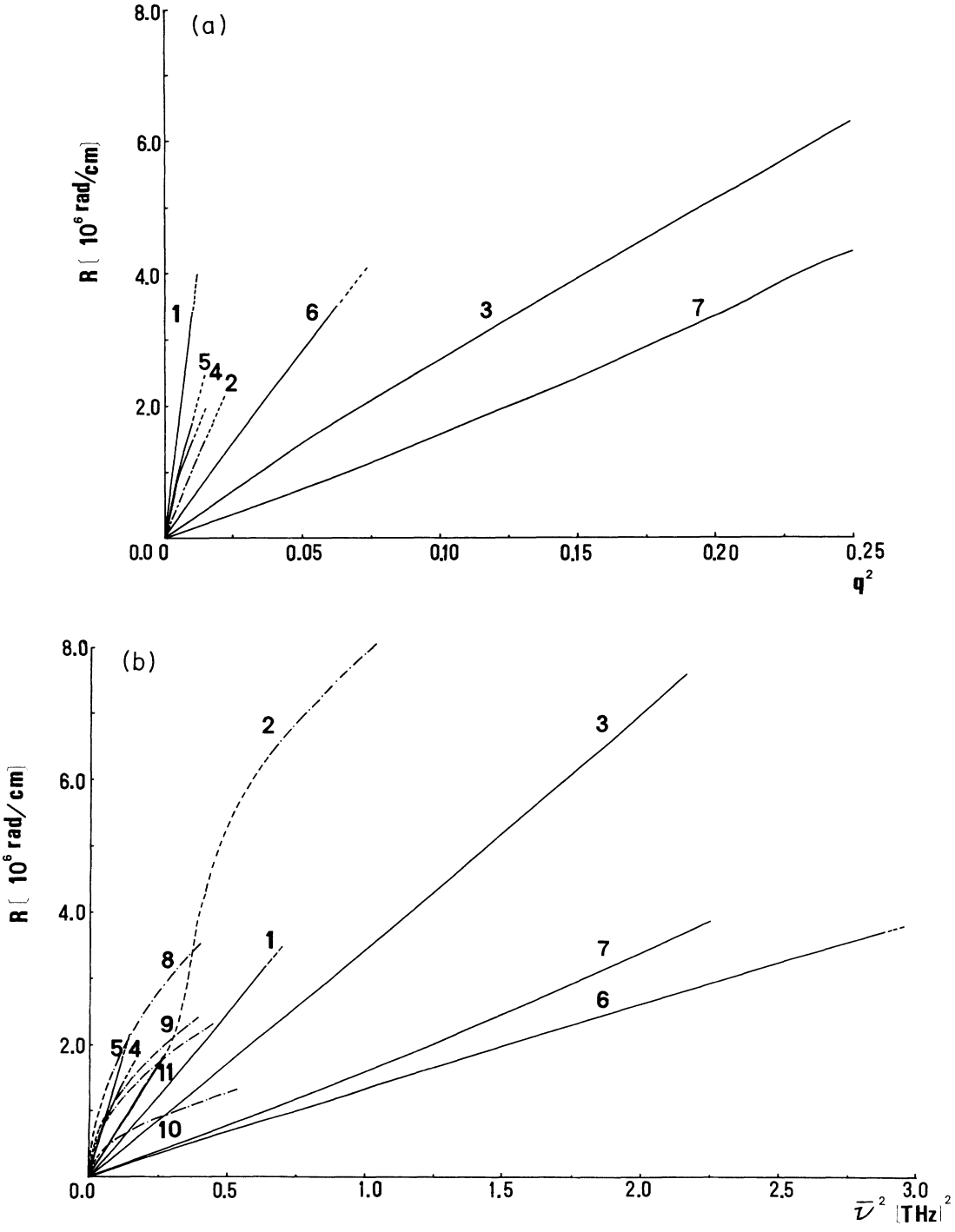

FIG. 4. Empirical ARP curves in the regime of q (a) or $\bar{\nu}$ (b), where the quadratic law of $\Delta\nu$ holds. The number attached to each of these curves corresponds to that in Fig. 3.

TABLE II. Experimental values of $V_{\pm}$ and their suitable limits.

Crystals	Te	$NaBrO_3$		$NaBr_{0.7}Cl_{0.3}O_3$	
No.	2	9	8	10	11
Axes	[001]	[001]	[111]	[111]	[001]
V_+ (10^5 cm/s)	1.68	2.41	2.40	1.93	2.16
V_-	1.18	1.86	1.68	1.74	1.74
$\bar{\nu}$ (THz)	0.8–1.0	0.25–0.6	0.3–0.6	0.3–0.65	0.3–0.7

$C_{ij}(\omega)$ is the tensor of ordinary Hooke's constants, and $d_{ij,l}(\omega)$ is the acoustic gyrotropic tensor, whose nonvanishing coefficients are present only in 21 noncentrosymmetric crystal classes.[5] In the PB theory, we have

$$C_{ij}(\omega,\mathbf{k})=C_{ij}+id_{ij,l}K_l, \quad (l=1,2,3) . \tag{2}$$

Substituting Eq. (2) in Christoffel's equations and solving for waves propagating along acoustic axes, we find the following:

(1) First-order spatial dispersion does not mix the longitudinal mode with the transverse modes, but couples the transverse modes with one another, which results in a rotation of the linearly-polarized plane and a velocity splitting

$$\Delta V_p=V_+-V_-\sim dk/\sqrt{\rho C} . \tag{3}$$

Its ARP, in analogy with the optical case, is defined as

$$R=\omega(1/V_--1/V_+)/2 =\pi Bv[1/v'_-(q)-1/v'_+(q)]/A , \tag{4}$$

where v is the incident frequency of the linearly-polarized wave measured, which is just equal to $\bar{\nu}$ of LCP and RCP phonons; ρ is the density; A is a lattice constant; B is a special constant; d and C are a certain set of the gyrotropic and Hooke's tensor, respectively. We have $A=c$, $B=1$, $C=C_{44}$, and $d=d_{45,3}$ for the [001] axes of the crystals measured; and for the [111] axes of cubic crystals, $A=a$, $B=\sqrt{3}$, $C=(C_{11}-C_{12}+C_{44})/3$, and $d=(d_{15,2}-d_{16,3}-d_{45,3})/3$.

(2) The frequency splitting is given by

$$\nu_{\pm}(q)=b_{\mathrm{I}}q\pm b_{\mathrm{II}}q^2/2 , \tag{5}$$

and so

TABLE III. Comparisons of sound velocities and their splittings in 10^5 cm/s units. ρ is the density, c (or a) is a lattice constant, and C_{ij} $(i,j=1,2,4)$ is the relative elastic constant obtained in standard microwave ultrasonic experiments. V_T is the velocity deduced from the experimental elastic constants C_{ij} $V_T^2=C/\rho$ [see the expositions of Eq. (4) in Sec. III (a)]. $\bar{V}$ is the average sound velocity observed in a suitable limit of q, i.e., $\bar{V}=(V_++V_-)/2$. $\Delta\bar{V}$ is the average velocity splitting in this suitable limit of q, i.e., $\Delta\bar{V}=(V_+-V_-)/2$. ΔV_P is the velocity splitting deduced from the PB theory [see Eq (3)], $\Delta V_P=d(k/2)(\rho C)^{1/2}$. Δq is the suitable limit of q, in which the slope of split curves may be roughly estimated by that of a straight line ($V_{\pm}$).

Crystals	α-SiO_2	Te	TeO_2	$Bi_{12}GeO_{20}$		$NaBrO_3$		$NaClO_3$	
c,a (Å)	5.405	5.924	7.612	10.15		6.70		6.576	
ρ (g/cm^3)	2.649	6.245	5.997	9.223		3.339		2.490	
C_{11} (10^{11} dyn/cm^2)				12.47		5.604		4.927	
C_{12}				3.70		1.790		1.463	
C_{44}	5.813	3.155	2.685	2.523		1.518		1.170	
No.	1	2	3	5		9	8	7	6
Axes	[001]	[001]	[001]	[100]	[111]	[100]	[111]	[100]	[111]
V_T	4.68	2.25	2.12	1.65	2.02	2.13	2.30	2.17	2.49
$\bar{V}$	4.68	2.28	2.17	1.68	2.00	2.13	2.04	2.16	2.49
$\Delta\bar{V}$	0.40	0.06	0.07		0.09	0.27	0.36	0.04	0.04
ΔV_P	0.38–0.53	0.02–0.08	0.04–0.08		0.07–0.10			0.02–0.05	0.03–0.05
Δq	0.05–0.07	0.02–0.07	0.10–0.20		0.04–0.06			0.10–0.30	0.05–0.10

$$\bar{\nu}(q)=b_{\mathrm{I}}q \ , \tag{6}$$

$$\Delta\nu(q)=b_{\mathrm{II}}q^2 \quad \text{or} \quad \Delta\nu(\bar{\nu})=b_{\mathrm{II}}\bar{\nu}^2/b_{\mathrm{I}}^2=\bar{b}_T\bar{\nu}^2 \ , \tag{7}$$

where $b_{\mathrm{I}}=V_TB/A$, $b_{\mathrm{II}}=\pi dB^2/\rho V_TA^2$, and $V_T^2=C/\rho$. Then, the $\nu_+(q)$ curve is gradually bending up from the straight line $\bar{\nu}(q)$ and $\nu_-(q)$ bending down from it, which are shown in Fig. 5(b). Consequently, the quadratic law of ARP will hold; that is,

$$R(q)=\frac{2\pi B}{A}\frac{b_{\mathrm{II}}q^2}{b_{\mathrm{I}}} \quad \text{or} \quad R(\bar{\nu})=\frac{2\pi B}{A}\frac{b_{\mathrm{II}}\bar{\nu}^2}{b_{\mathrm{I}}^3} \ . \tag{8}$$

Although the quadratic law of $\Delta\nu$ holds in different regimes of q or $\bar{\nu}$ for most crystals measured, Eq. (5) is not agreeable with all curves shown in Fig. 2, except that of TeO_2. Therefore, we deduced a few empirical formulas below to fit with our experiment results. First, the dispersion relations of LCP and RCP phonons may be generally written as

$$\nu_\pm(q)=b_1^\pm q+b_2^\pm q^2+b_3^\pm q^3+\cdots \ , \tag{9a}$$

and so

$$\Delta\nu(q)=(b_1^+-b_1^-)q+(b_2^+-b_2^-)q^2+(b_3^+-b_3^-)q^3+\cdots \ , \tag{9b}$$

$$2\bar{\nu}(q)=(b_1^++b_1^-)q+(b_2^++b_2^-)q^2+(b_3^++b_3^-)q^3+\cdots \ . \tag{9c}$$

For a simple estimation, the terms of q^3 and higher-order powers in Eqs. (9) may be negligible in the range where $\Delta\nu=bq^2$ (or $\bar{b}\bar{\nu}^2$) holds. So we have $b_1^+=b_1^-=b_1$, $b_2^+-b_2^-=b$, and

$$\nu_\pm(q)=b_1q+(b_0\pm b)q^2/2 \ , \tag{10}$$

$$\bar{\nu}(q)=b_1q+b_0q^2/2 \ , \tag{11}$$

where $b_0=b_2^++b_2^-$. Then, the $\nu_-(q)$ curves are close to a straight line of $|b_0|=b$ and the $\nu_+(q)$ curves are bending up when $b_0>0$, which are consistent with the curves of α-SiO_2, $Bi_{12}GeO_{20}$, and $NaClO_3$ in the [111] direction. On the contrary, the $\nu_+(q)$ curves are close to this straight line, and the $\nu_-(q)$ curves are bending down when $b_0<0$, which are consistent with the curves of Te and $NaClO_3$ in the [001] direction. Clearly, the empirical curves $\nu_\pm(q)$ for $b_0=0$ are consistent with the PB curves, which are close to the curves of TeO_2. These results are shown in Fig. 5(c)–5(h) for different b_0, where the $\bar{\nu}(q)$ and $\nu_\pm(q)$ curves are indicated by the dot-dashed and the solid lines, respectively. A schematic diagram for the crystals not exhibiting AA is shown in Fig. 5(a) for comparison, which illustrates how spatial dispersion might affect the shape of TA branches. Consequently, the empirical expression of ARP in this range is approximately given by

$$R(q)=\frac{2\pi B}{A}\frac{bq^2}{b_1+2b_0q+(b_0^2-b^2)q^2/b_1}$$

or (12)

$$R(\bar{\nu})=\frac{2\pi B}{A}\frac{b\bar{\nu}^2}{b_1^3+2b_0b_1\bar{\nu}-b^2\bar{\nu}^2/b_1} \ .$$

Evidently, Eqs. (10), (11), and (12) will be equivalent to

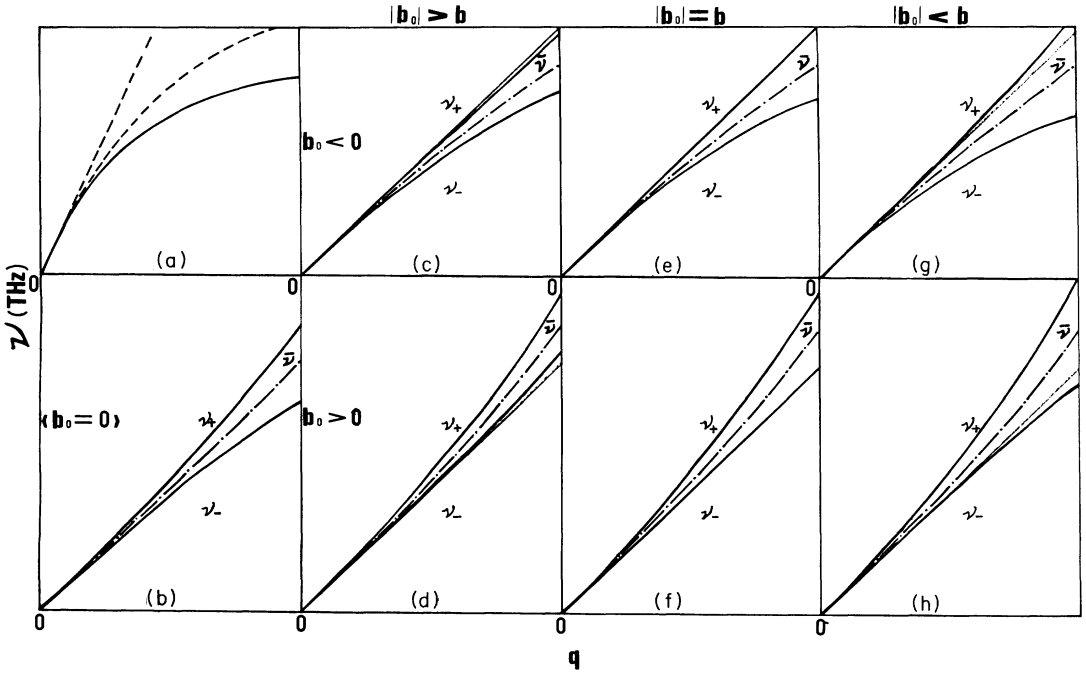

FIG. 5. Empirical split curves in the same regime as that in Fig. 4. (a) Schematic diagram in the absence of AA; (b) the PB curve and the empirical curve of $b_0=0$; (c)–(b) the empirical curves for different b_0.

Eqs. (5), (6), and (8) when $b_0=0$ and q (or $\bar{\nu}$) approaches zero, respectively. The fitted data show $b_1 \sim b_I$ and $\bar{b} \sim b/b_1^2$, but $b_0 \neq 0$ (see Table I). With further increase of q or $\bar{\nu}$, the quadratic law of ARP will no longer hold owing to the additional terms of the denominator in Eq. (12), even though $\Delta\nu = bq^2$ or $\bar{b}\bar{\nu}^2$ still holds.

For larger q, the q^3 and higher-order terms in Eqs. (9) will not be negligible, and their composite contribution to acoustical activity of crystals is probably negative; for example, $\Delta\nu$ will be decreased by a term of q^4 when the anharmonicity as a perturbation has been taken into account (see Ref. 6).

Thus it can be seen that the exhibition of the effect of rotation of the polarization plane of TA waves propagating along an acoustic axis in crystals lacking certain symmetry elements and the varying law of AA in the long-wavelength approximation as a function of q or $\bar{\nu}$ have been predicted theoretically by Portigal and Burstein and confirmed experimentally by Pine *et al.* (see Refs. 1–11). The contribution of our inelastic-neutron-scattering experiments to the study on AA of crystals is mainly to reveal further AA behavior of the short-wavelength phonons, which is different from that of the long-wavelength phonons. However, at present, the theory of AA cannot yet provide satisfactory estimates of the regime of q or $\bar{\nu}$ where the long-wavelength approximation is suitable, which may be different for different crystals, and theoretical explanations of AA behavior in the regime of larger q or $\bar{\nu}$. Moreover, the experimental fact that the quadratic law of $\Delta\nu$ holds in TeO_2 and $NaClO_3$ up to their Brillouin-zone boundary cannot be considered as being in agreement with the PB theory. It is difficult to give a reasonable explanation. The unexpected AA behavior of $NaBrO_3$ is also not easy to understand.

(b) It has been known that OA is related to the chirality of the crystal structure; the sense of rotation of polarized light is traced to the hand of the specific helices of atoms arranged along propagation direction, and its magnitude will be determined by the characteristic of this helix (some specific distances between atoms, their numbers, and electronic polarizabilities).[14] Our experiments show that this rule is possibly applicable to AA. Naturally, AA is also the macroscopic response to the existence of a certain symmetric or nonsymmetric spatial helix structure. The symmetric structural helix is defined as a perfectly regular helix of atoms with the chirality of the screw axis in the space group, and the nonsymmetric one is a helix of atoms that is not perfectly regular and has a chirality independent of that of the space-group helices.

TABLE IV. Magnitude of other effects of first-order spatial dispersion on the propagation velocity of acoustic waves in the [110] direction of cubic crystals and the [100] direction of uniaxial crystals.

Crystal	Group	Coupling	ΔV_g (in cgs units)
Cubic	O-432	TA_1-TA_2	$\dfrac{(d_{15,2}K)^2}{4\sqrt{\rho}\lvert(C_{11}-C_{12})\sqrt{C_{44}}-C_{44}\sqrt{2(C_{11}-C_{12})}\rvert}$
	T_d-$\bar{4}3m$	LA-TA_1	$\dfrac{[(d_{14,1}+d_{15,2})K]^2}{4\sqrt{\rho}\lvert(C_{11}+C_{12}+2C_{44})\sqrt{C_{44}}-C_{44}\sqrt{2(C_{11}+C_{12}+2C_{44})}\rvert}$
	T-23 C_4-4 S_4-$\bar{4}$	LA-TA_1-TA_2	
Tetragonal	D_4-422 D_{2d}-$\bar{4}2m$	TA_1-TA_2	$\dfrac{(d_{46,2}K)^2}{2\sqrt{\rho}\lvert C_{44}\sqrt{C_{66}}-C_{66}\sqrt{C_{44}}\rvert}$
	C_{4v}-4mm C_{6v}-6mm	LA-TA_1	$\dfrac{(d_{15,1}K)^2}{2\sqrt{\rho}\lvert C_{11}\sqrt{C_{44}}-C_{44}\sqrt{C_{11}}\rvert}$
Hexagonal	C_{3h}-6 D_{3h}-6m2	LA - TA_2	$\dfrac{(d_{12,2}K)^2}{4\sqrt{\rho}\lvert(C_{11}-C_{12})\sqrt{C_{11}}-C_{11}\sqrt{2(C_{11}-C_{12})}\rvert}$
	C_6-6	LA-TA_1-TA_2	
Trigonal	D_6-622 D_3-32	TA_1-TA_2	$\dfrac{[(d_{14,1}+d_{15,2})K]^2}{4\sqrt{\rho}\lvert(C_{11}-C_{12})\sqrt{C_{44}}-C_{44}\sqrt{2(C_{11}-C_{12})}\rvert}$
	C_3-3 C_{3v}-3m	LA-TA_1-TA_2	

It appears that the point-group symmetry proposed by the PB theory should determine the possibility of the existence of AA in crystals, and the chirality of the arrangement of atoms along wave propagation directions and the interactive forces between them should be responsible for the size, sense, and variation of AA. This empirical rule has been theoretically demonstrated in simple lattices with central forces.[6]

(c) Abrahams *et al.* found that the optical rotatory power of $NaBr_xCl_{1-x}O_3$ is decreased from 2.61 to 1.99 or 3.55 to 2.43 (deg/mm) when the composition x is changed from 1.0 to 0.9 or 0.0 to 0.2 at 5461 Å.[15] Our experiments show that its ARP is also decreased in both the [001] and the [111] directions when x is changed from 1.0 to 0.7. Therefore, the special composition at which the rotatory power is zero may be different for AA and OA because of their difference in the changes with x. In other words, AA may not appear in certain crystals which will exhibit OA or vice versa. In addition, similar to the status of the component magnetizations of the two sublattices with opposite orientations, one may expect a switching of the sign of ARP, or (and) and a jump of its magnitude in certain solid solution single crystals consisting of two isostructural compounds as a function of q (perhaps temperature and pressure as well) when q goes through a specific value, which may be a function of the composition x, because of the opposite senses and different q dependences in AA of the two crystals.

(d) In general directions, the spatial dispersion will also contribute terms in the dynamical matrix of sound waves. Our results calculated using the PB theory for all noncentrosymmetric crystal classes possessing axes of threefold or higher symmetry manifest that in any classes having vanishing $d_{45,3}$ the first-order spatial dispersion does not affect the propagation of sound waves in degenerate directions. In nondegenerate directions, the solutions of secular equations may be divided into two kinds; one of them results from the coupling of three acoustical vibration modes (LA-TA1-TA2). The other, similar to Aa, is that one mode retains the linearly-polarized and the other two modes (TA1-TA2 or LA-TAm) are coupled with each other. The coupling of TA1-TA2, by analogy with OA, will decompose the linearly polarized waves into right- and left-elliptically-polarized modes having different velocities and the coupling of LA-TA will lead to modes in which the polarization vector "rolls" along the direction of propagation. Their velocities are changed as $V_s = V_s(0) + \Delta V_s$ $(s=1,2)$, where $V_s(0)$ are those in the absence of spatial dispersion, and the velocity splitting is estimated roughly to be $\Delta V_g = \Delta V_1 + \Delta V_2 \sim (dk)^2/C\sqrt{\rho C}$, (see Table IV). Then, we have $\Delta V_g/\Delta V_p \sim dk/C$ from the consideration of Eq. (3). Our calculations show the order of magnitude of $d \sim 10^{3\pm1}$ cgs units (see Table I). It follows that the measurements for the elliptical polarization or rolling effects by means of inelastic neutron scattering is more difficult than that for the circularly-polarized acoustic waves. At least, they have not been verified definitely by any physical experiment so far.

The effects of spatial dispersion on the optical phonons are not involved in our experiments for technical reasons. They may be observed in either the infrared absorption spectra or the Raman-scattering spectra. A much more detailed study of this subject must await parallel attention and greater effort in theoretical condensed-matter physics.

ACKNOWLEDGMENTS

We are grateful to Professor Li Yin-yuan, Professor Zhang Zong, Professor Pu Fu-que, and Professor Tang Di-Sheng of the Institute of Physics of the Academia Sinica, Professor J. Joffrin of the University Paris–Sud, and Dr. B. Hennion of Laboratory Léon-Brillouin for many illuminating discussions and advice. And we would like to thank our colleagues Professor Yan Qi-wei, Professor Zhang Ban-lin, Professor Zhang Tai-yong, Professor Niu Shi-wen, and Professor Gou Cheng for their kind help, as well as Ma Wen-yi for the preparation of single crystals measured.

[1]A. A. Andronov, Izv. Vyssh. Uchebn. Zaved. Radiofiz. **3**, 645 (1960); V. P. Silin, Zh. Eksp. Teor. Fiz. **38**, 977 (1960); R. A. Toupin, Arch. Ration. Mech. Anal. **11**, 385 (1962); G. Kluge *et al.*, Acustica **16**, 60 (1965); Phys. Status Solidi **17**, 109 (1966).

[2]D. L. Portigal and E. Burstein, Phys. Rev. **170**, 673 (1968).

[3]E. Moritz, Mol. Cryst. Liq. Cryst. **49**, 7 (1978).

[4]V. K. Wadhawan, Acta Crystallogr. Sect. A **35**, 629 (1979); Phase Transitions **3**, 3 (1982); K. V. Bhagwat *et al.*, *ibid.* **4**, 19 (1983).

[5]K. Kumaraswamy *et al.*, Acta Crystallogr. Sect. A **36**, 760 (1980); Indian J. Pure Appl. Phys. **20**, 135 (1982); J. Acoust. Soc. Am. **73**, 418 (1983); B. V. Bokut, *et al.*, Kristallografiya **29**, 802 (1984) [Sov. Phys. Crystallogr. **29**, 475 (1984)]; C. Mei and B. Hao, Common. Theory. Phys. (China) **4**, 795 (1985).

[6]Y. Li and L. Chen, Phys. Rev. B **36**, 9507 (1987).

[7]M. M. Elcombe, Proc. Phys. Soc. London **91**, 947 (1967).

[8]A. S. Pine *et al.*, Phys. Rev. **188**, 1489 (1969); Phys. Rev. B **2**, 2049 (1970); J. Acoust. Soc. Am. **49**, 1062 (1971).

[9]J. Joffrin and A. Levelut, Solid State Commun. **8**, 1573 (1970); H. Bialas and G. Schauer, Phys. Status Solidi **72**, 679 (1982).

[10]B. M. Powell and P. Martel, Bull. Am. Phys. Soc. **15**, 810 (1970); J. Phys. Chem. Solids **36**, 1287 (1975); W. C. Hamilton *et al.*, *ibid.* **35**, 1089 (1974).

[11]C. Joffrin *et al.*, J. Phys. (Paris) Lett. **41**, 391 (1980).

[12]C. Lin *et al.*, Solid State Commun. **54**, 803 (1985);

[13]Q. Lin *et al.*, Phys. Rev. Lett. **58**, 2095 (1987).

[14]A. M. Glazer and K. Stadnicka, J. Appl. Crystallogr. **19**, 108 (1986).

[15]S. C. Abrahams *et al.*, Solid State Commun. **24**, 515 (1977).